HHS Public Access

Author manuscript

Biomaterials. Author manuscript; available in PMC 2017 July 01.

Published in final edited form as:

Biomaterials. 2016 July ; 93: 1–9. doi:10.1016/j.biomaterials.2016.03.032.

An iTEP-salinomycin nanoparticle that specifically and effectively inhibits metastases of 4T1 orthotopic breast tumors

Peng Zhao[1], **Guiquan Xia**[2], **Shuyun Dong**[1], **Zhaong-Xing Jiang**[2], and **Mingnan Chen**[1,*]

[1] Department of Pharmaceutics and Pharmaceutical Chemistry, University of Utah, Salt Lake City, Utah 84112, U.S.A

[2] School of Pharmaceutical Sciences, Wuhan University, Wuhan, Hubei 430071, China

Abstract

Cancer stem cell (CSC) inhibitors are a new category of investigational drugs to treat metastasis. Salinomycin (Sali) is one of most studied CSC inhibitors and has reached clinical tests. Several drug carriers have been developed to improve efficacy of Sali. However, Sali has not been shown to inhibit metastasis from orthotopic tumors, the gold standard for metastasis. To fill this gap, we developed an immune-tolerant, elastin-like polypeptide (iTEP)-based nanoparticle (iTEP-Sali-ABA NP) that released 4-(aminomethyl)benzaldehyde-modified Sali (Sali-ABA) under acidic conditions. We found that the NP increased the area under the curve (AUC) of Sali-ABA by 30-fold and the tumor accumulation by 3.4-fold. Furthermore, no metastasis was detected in any of the mice given the NP. However, all the mice died of primary tumor burdens. To overcome primary tumor growth and improve the overall survival, we applied a combination therapy consisting of the iTEP-Sali-ABA NP and iTEP NP-delivered paclitaxel. This therapy effectively retarded primary tumor growth, and most importantly, improved the overall survival. In conclusion, delivery of Sali-ABA by the NP, alone or in combination with paclitaxel, was more effective than free Sali-ABA in decreasing metastasis and increasing survival. This iTEP-Sali-ABA NP represents a novel and clinically promising therapy to combat metastasis.

Keywords

metastasis; cancer stem cell; salinomycin; immune-tolerant elastin-like polypeptides (iTEP) nanoparticle; breast cancer

1. Introduction

Although there have been tremendous advances in breast cancer treatment, treatment for metastatic breast cancer remains problematic. In particular, breast cancer patients who have distant metastasis still face a poor prognosis [1-3]. Therefore, effective treatments to cure or

*Corresponding author: Mingnan Chen, Mingnan.chen@utah.edu.

prevent metastasis are of great interest. A focal point among efforts to identify effective anti-metastasis therapies is cancer stem cells (CSCs) because these cells play important roles in initiating and promoting metastases [4-7]. Since CSCs are resistant to conventional chemotherapeutics and radiotherapeutics [8-10], there is an immediate need to discover CSC-specific inhibitors.

Salinomycin (Sali) was discovered as a selective inhibitor of CSCs, and clinical data support its inhibitory effect to human breast cancer [11, 12]. Sali was shown to decrease the tumor-seeding ability and metastasis-forming ability of murine 4T1 breast tumor cells [11]. In addition, Sali reduced metastatic burdens when it was injected concurrently with the tumor cells intravenously, a simple metastasis model with minimal clinical relevance [13]. Sali also resulted in partial regression in all breast cancer patients tested (n=5) [12], which underscores the clinical significance of this inhibitor. However, Sali has not yet been demonstrated to inhibit metastasis from established and clinically relevant orthotopic breast tumors. This inhibition requires the accumulation of Sali in primary tumors and metastases to eliminate CSCs. Furthermore, Sali is toxic to healthy tissue [14-16], and its medical usage would be benefited by a delivery strategy that limits the accumulation in healthy tissue. To meet these two needs of the biodistribution of Sali, a delivery system is needed to modulate the biodistribution. To this end, we and others have developed several types of delivery systems that help to increase accumulation of Sali in tumors through the enhanced permeability and retention effect (EPR) and active targeting [2, 17-19]. However, none of these systems has shown a capacity that enables Sali to inhibit metastasis from orthotopic tumors. Therefore, we aimed to develop a carrier to improve Sali's efficacy and achieve inhibition of metastasis of orthotopic breast tumors.

We have previously delivered Sali as an encapsulated form in carriers, which did not lead to an inhibition of metastasis [2]. These carriers might be improved by incorporating a controlled release mechanism, such as linking Sali and the carriers through a cleavable covalent bond. These carriers with the controlled release mechanism may have the capability of improving the pharmacokinetics and biodistribution of Sali over encapsulated Sali [2]. These improvements may further lead to more Sali accumulations in tumors, a stronger CSC-killing effect, and ultimately a stronger metastasis-inhibition effect.

To generate the new carrier for Sali, we first modified Sali by attaching a pH-sensitive linker, 4-(aminomethyl)benzaldehyde (ABA), to Sali's carboxylic group. This modified Sali, Sali-ABA, was then conjugated to our recently invented, immune-tolerant elastin-like polypeptides (iTEPs) to create iTEP-Sali-ABA [20]. Sali-ABA was confirmed to be released from the iTEP in a pH-dependent manner, and iTEP-Sali-ABA conjugates were selectively toxic to CSCs. The iTEP-Sali-ABA conjugates self-assembled into a NP, and the Sali-ABA delivered by this NP had better pharmacokinetics and tumor accumulation profiles than free Sali-ABA. This NP was found to inhibit metastasis but did not stop tumor growth. To address this limitation, a combination therapy was designed to target both primary tumor growth and metastasis. A conventional chemotherapeutical, paclitaxel (PTX), primarily targets differentiated tumor cells and was encapsulated into the NP (termed PTX NP). This combination therapy of two NPs is designed to inhibit both metastasis (by iTEP-Sali-ABA NP) and primary tumor growth (by PTX NP). The combination therapy inhibited tumor

growth, and more importantly, showed a significant improvement in the inhibition of metastasis. Together, these effects produced a longer survival than the iTEP-Sali-ABA NP monotherapy.

2. Materials and Methods

2.1 Materials

All chemicals, unless otherwise described, were purchased from Thermo Fisher Scientific Inc. (MA, USA) at biological grade. Organic solvents including acetonitrile (ACN), Dichloromethane (DCM), Dimethylformamide (DMF), isopropanol, and methanol were purchased from Thermo Fisher Scientific Inc. (MA, USA) at HPLC grade. The LB and TB media were prepared in our lab using the standard formula [21]. All the cell culture plates were purchased from Corning Inc. (NY, USA). The cell culture media and supplements including RPMI-1640 (with 2mM L-Glutamine), and fetal bovine serum (FBS) were purchased from Life Technologies, Inc. (CA, USA).

4T1, a highly metastatic murine cell line derived from a spontaneous syngeneic breast cancer of Balb/c mice were purchased from American Type Culture Collection (MD, USA). 4T1-luc, a 4T1 cell line that stably expressed firefly luciferase was generated in-house using a published method [22]. 293T, a human embryonic kidney epithelial cell line, MDA-MB-231, a human metastatic breast cancer cell line, HCT-15, a human colorectal adenocarcinoma cell line, and PC-3, a human prostate adenocarcinoma cell line were all from American Type Culture Collection.

4T1, 4T1-luc, HCT-15, and PC-3 cells were maintained in monolayer cultures in an RPMI 1640 medium supplemented with 10% FBS. Cells were maintained at 37 °C humidified atmosphere with 5% CO_2. 293T and MDA-MB-231 cells were maintained in monolayer cultures in a DMEM medium supplemented with 10% FBS. Cells were maintained at 37 °C humidified atmosphere with 5% C O_2.

Female Balb/c mice that were 24-28 days old (18-19 g) were purchased from Charles River Laboratories International, Inc. (USA). All the animal experiment protocols were approved by the Institutional Animal Care and Use Committee at the University of Utah (14-11005).

2.2 Synthesis of Sali-ABA

Sali (9.50 g, 12.67 mmol), (4-(1,3-dioxolan-2-yl)phenyl)methanamine (3.40 g, 18.97 mmol), and 1,3-diisopropylcarbodiimide (2.39 g, 18.97 mmol) were first dissolved together in 150 mL dry DCM. To this stirred mixture, 1-hydroxybenzotriazole (2.05 g, 15.17 mmol) solubilized in 10 mL of dry DMF was added at 0 °C. The resulted mixture was further stirred for 24 h before allowed to warm to room temperature. Then, the mixture was stirred for additional 24 h. The mixture was then quenched with 200 mL brine, and reaction products and unused reactant were extracted three times with 100 mL DCM. The combined DCM solution was dried over anhydrous Na_2SO_4, concentrated under vacuum, and the residue was purified by flash chromatography on silica gel (200-300 mesh). The purified conjugation product was a white solid.

To de-protect the aldehyde group of the conjugation product (Sali-ABA), the product was dissolved in 22 mL THF to which 2 N HCl (22.72 mL) was added. The mixture was stirred at room temperature for 6 h. Then the reaction was quenched with aqueous $NaHCO_3$ (200 mL) and extracted with DCM (100 mL, two times). The combined DCM solution was dried over anhydrous Na_2SO_4, concentrated under vacuum. The residue was purified by flash chromatography on silica gel (200-300 mesh). The purified, de-protected Sali-ABA was a white solid (6.68 g, 61% yield). The presence of Sali-ABA was confirmed by the ^1H NMR. The ^1H NMR was performed in $CDCl_3$ and measured on a Bruker 400 MHz. The chemical shift was analyzed and integrated. ^1H NMR ($CDCl_3$, 400 MHz) δ 0.75-0.81 (m, 4H), 0.81-0.86 (m, 5H), 0.86-0.91 (m, 6H), 0.91-0.99 (m, 8H), 1.14 (s, 3H), 1.19-1.27 (m, 8H), 1.46-1.55 (m, 4H), 1.80-1.88 (m, 5H), 2.02-2.06 (m, 1H), 2.18-2.45 (m, 2H), 2.62-2.73 (m, 1H), 2.74-3.13 (m, 8H), 3.37-3.47 (m, 1H), 3.53 (s, 1H), 3.60-3.84 (m, 6H), 3.85-3.95 (m, 1H), 4.03-4.20 (m, 3H), 4.43-4.59 (m, 1H), 4.63-4.78 (m, 1H), 6.23-6.29 (m, 1H), 6.63-6.77 (m, 1H), 7.14 (d, J = 4.0 Hz, 1H), 7.52 (d, J = 8.0 Hz, 2H), 7.81 (d, J = 8.0 Hz, 2H), 9.95 (s, 1H). For ESI-MS analysis, purified reaction product was dissolved in a 50% acetonitrile aqueous solution containing 0.1% TFA, loaded onto a sinapinic acid matrix, and examined using a QTOF 2 Mass Spectrometer (Waters, MA, USA) equipped with a nitrogen laser (337 nm).

2.3 Synthesis of Sali-ABA-MPBH

Under the atmosphere of argon, a mixture of Sali-ABA (1.70 g, 1.96 mmol), MPBH-HCl (0.91 g, 2.97 mmol), and 4 Å molecular sieve (1 g) in dry isopropanol/methanol (20 mL/20 mL) was prepared and stirred at 40 °C overnight. After the mixture was filtered and the solvent was evaporated, the residue was purified by flash chromatography on silica gel (200-300 mesh). The purified conjugation product was a light yellow solid. The yield was 41%. The purity of the collected conjugation product was confirmed by HPLC. The presence of Sali-ABA-MPBH conjugates was confirmed by the ^1H NMR. The ^1H NMR was performed in $CDCl_3$ and measured on a Bruker 400 MHz. The chemical shift was analyzed and integrated. ^1H NMR ($CDCl_3$, 400 MHz) δ 0.76-0.82 (m, 4H), 0.82-0.87 (m, 6H), 0.87-0.93 (m, 8H), 0.93-1.00 (m, 7H), 1.14 (s, 3H), 1.19-1.27 (m, 11H), 2.01-2.07 (m, 5H), 2.17-2.36 (m, 3H), 2.63-2.77 (m, 6H), 2.77-3.13 (m, 8H), 3.37-3.53 (m, 2H), 3.53-3.63 (m, 1H), 3.64-3.74 (m, 2H), 3.75-3.84 (m, 2H), 3.86-3.97 (m, 1H), 4.05-4.19 (m, 3H), 4.22-4.32 (m, 1H), 4.36-4.51 (m, 1H), 4.56-4.73 (m, 1H), 6.20-6.32 (m, 1H), 6.45-6.60 (m, 1H), 6.81-6.90 (m, 2H), 7.05-7.13 (m, 1H), 7.20-7.28 (m, 2H), 7.30-7.41 (m, 4H), 7.45-7.54 (m, 2H), 7.69 (s, 1H), 9.38-9.62 (m, 1H). The reaction product was analyzed by ESI-MS as described above.

The formation of the hydrazone bond between Sali-ABA and MPBH-HCl is extremely slow at room temperature. Only a trace of the product can be detected after 48 h of reaction at this temperature. To address this issue, the reaction temperature was raised to 40 °C and molecular sieves were added to promote this reaction.

2.4 Expression and purification of iTEP

The gene that codes the iTEP was generated as previously described. The production and purification of the iTEP were same as previously described [2].

2.5 Synthesis of iTEP-Sali-ABA

iTEP-Sali-ABA was synthesized as previously described [2]. TCEP-reduced iTEP was reacted with Sali-ABA-MPBH in phosphate buffer (pH=7.00, 1 M NaPO4, 1 mM EDTA). After purification, the purity of iTEP-Sali-ABA conjugate was confirmed by HPLC. After the purification, iTEP-Sali-ABA conjugate was lyophilized and stored at −20 °C. The conjugation efficiency of Sali-ABA to iTEP was determined by the Ellman's reagent method. To this end, 5,5'-Dithiobis-(2-Nitrobenzoic Acid) (DTNB; Ellman's Reagent, Thermo Fisher Scientific Inc., Massachusetts, USA) was used to quantify the conjugation ratio by measuring the number of thiol groups. The quantification was done following the manufacturer's protocol, and the concentration of thiol groups was determined by fitting data to a standard curve of a series of cysteine solutions at different concentrations. The absorption was measured at 410 nm.

2. 6 Loading of PTX into iTEP-Sali-ABA NP

PTX was loaded into iTEP-Sali-ABA NP as previously described [2]. 10 mg iTEP-Sali-ABA, 5 mg PTX, and 2.5 mg α-Tocopherol (Sigma–Aldrich, MO, USA) were co-dissolved in 125 μL DMF. The encapsulated PTX was determined by HPLC based on its absorbance at 280 nm and a standard curve of PTX. The standard curve was generated by measuring the absorbance of serially diluted PTX on HPLC. The column for HPLC was Symmetry C18 column (100 Å, 3.5 μm, 4.6 mm × 150 mm, Waters, MA, USA) which was connected to an Agilent Infinity-1260 LC system (CA, USA). The analysis was performed using water (solvent A) and Acetonitrile (solvent B) (0.05% TFA) at a flow rate of 1.0 mL/min. The gradient was gradually increased from 80% B to 100% B from 0 to 20 minutes. The loading efficiency was defined by the following equation:

$$\text{Loading efficiency } (\%) = 100 \times (\text{PTX encapsulated}) / (\text{PTX feed}).$$

2.7. Dynamic light scattering (DLS) measurement

The measurement was carried out as previously described [2]. iTEP, iTEP-Sali-ABA conjugate, or PTX NP were measured at 25 μM in PBS at 37°C using a Malvern Zetasizer Nano system (Malvern, Chester County, PA, USA).

2.8. *In vitro* Sali-ABA release assay

The release of Sali-ABA from iTEP-Sali-ABA NP was measured after the NP was incubated in PBS (pH=7.4) or 0.1M Sodium acetate/Acetic acid buffer (pH=5) at 37 °C. Multiple repeats of each mixture were kept in separate Eppendorf tubes and shaken at 100 rpms at 37 °C. At predetermined time points, fr ee Sali-ABA in one tube of sample was determined by HPLC based on a standard curve of Sali-ABA. The standard curve was established at 280 nm. The HPLC setup was the same as the described in the section 2.6.

The relationship of the percentage of Sali-ABA release (F) with time (t) was fitted using the following equation and GraphPad V5.0.

$$F_{\%,released}=100\left[1-e^{-Kt}\right]$$

K is the release rate constant:

$$K=\frac{\ln 2}{t_{1/2}}$$

2.9 *In vitro* PTX release assay

The *in vitro* release profile of PTX from the PTX NP was measured by a previously described dialysis method with minor modifications [18]. The PTX NP was diluted in 0.5 mL MiliQ water containing 4% BSA and kept in a bag (Spectrum Laboratories, Inc. CA, USA, MW cutoff = 8,000 Da). The bag was dialyzed in 100 mL PBS solution (pH=7.4) and shaken at 100 rpms at 37 °C. At predetermined time points, 10 μL of the sample was collected form the bag after the sample was well mixed. PTX in the 10 μL sample was determined by HPLC as described in the section 2.6 and assumed to be un-released PTX. The release kinetics was determined as described in the section 2.8.

2.10 Pharmacokinetics and biodistribution study

Sali-ABA concentrations in blood and tissues were analyzed, and the concentrations were analyzed as previously described [2].

2.11 Cytotoxicity studies

The cytotoxicity was measured as previously described [2]. The incubation time was 72 hours. 4T1-lu [2], HCT-15 [23], MDA-MB-231 [24], and PC-3 [25] mammosphere cells were generated as the previously described and used as the CSC models of the corresponding tumors.

2.12 Tumor growth study

Balb/c mice were inoculated subcutaneously with 10^6 4T1-luc cells in 50 μL PBS at the #9 mammary glands. At the 7^{th} day after inoculation when the volumes of all tumors reached or exceeded 100 mm^3, the mice were randomly assigned into groups as described in Figure 5 and 6. The dosing and dosing schedules are as following:

1. PBS control (three day interval), 7 mice
2. Sali-ABA (20 mg/Kg BW, three-day interval), 7 mice
3. iTEP-Sali-ABA NP (20 mg/Kg BW, three-day interval), 6 mice
4. PTX NP (10 mg/Kg BW, three-day interval), 6 mice
5. PTX NP and iTEP-Sali-ABA combination, iTEP-Sali-ABA NP on the first day (20 mg/Kg BW), PTX NP on the second day (10 mg/Kg BW), then two-day interval; 14 mice

Seven total doses were administered intravenously. The length and width dimensions of tumors were measured with a caliper every other day. Tumor volumes were estimated using the formula: Tumor Volume = (length × width^2/2) [18]. Also, mouse body weight was recorded the same day when the tumor size was measured. The treatments of PTX NP and the combination therapy were done after we obtained results of the first three treatment groups.

Moreover, in order to monitor metastasis, bioluminescence signals released from 4T1-luc cells were monitored as previously described [22]. Specifically, experimental mice were injected intraperitoneally with 100 μl of D-luciferin (15 mg/ml) at predetermined time points (twice each week, 3-4 days interval). At 15 minutes after luciferin injection, the mice were imaged under anesthesia in a Xenogen IVIS 200 biophotonic imager (PerkinElmer, Inc., MA, USA). The bioluminescence intensity was denoted using photon emission from the subject or radiance in the unit of photons/sec/cm^2/sr (steradian). We set the intensity scale for all bioluminescence images between 1×10^6 photons/sec/cm^2/sr and ~1×10^7 photons/sec/cm^2/sr. Our criterion of metastasis was that an area with a pre-defined size and outside of primary tumors had a metastasis if the average radiance of this area exceeded 1×10^6 photons/sec/cm^2/sr. We designated the number of days between tumor inoculation and the first day that we observed metastasis on a mouse as the metastasis-free survival time. Mice were sacrificed according to preapproved endpoints by the IACUC. The overall survival time was counted as days between tumor inoculation and mouse sacrifice. Metastasis-free survival and overall survival were analyzed by the Kaplan-Meier method, and the median survival of each groups were compared using the Log-rank test with GraphPad V5.0.

3. Results

3.1 Synthesis and characterization of Sali-ABA and Sali-ABA-MPBH conjugates

In order to link Sali to iTEP through a cleavable chemical bond, we first modified Sali by attaching a small molecule, ABA, to it. The resultant Sali-ABA was then connected to a bifunctional linker, MPBH to produce a cleavable hydrazone bond (Figure 1A). Last the conjugate, Sali-ABA-MPBH, was linked to iTEP.

After the Sali-ABA conjugation product was purified, we used HCl to remove a protecting group of ABA and generate an active aldehyde group on the product. The MS spectrum of this de-protected product confirmed that it was our expected conjugate, Sali-ABA (Figure 1B). The yield for the de-protected Sali-ABA was 61%.

Sali-ABA and MPBH were linked together through an aldehyde group and a hydrazide group on the two molecules (Figure 1A). MS spectrum (Figure 1C) and ^{1}HNMR peak data (Materials and Method) of the purified conjugation product indicated that the Sali-ABA-MPBH formed in the reaction. The yield of Sali-ABA-MPBH was 41%.

We compared the toxicity of Sali-ABA and Sali to regular 4T1-luc tumor cells (Figure 2A). Toxicity of Sali-ABA was significantly lower than Sali. The IC_{50} value of Sali-ABA was 16.4 μM (95% CI=14.3~18.8 μM); the IC_{50} value of Sali was 4.4 μM (95% CI=2.3~11.2

μM). The lower toxicity of Sali-ABA agreed with its higher tolerated dose in mice as compared to Sali alone (Data not shown). We then compared the toxicity of Sali-ABA to regular 4T1-luc cells and to cells collected from 4T1-luc mammospheres. Mammosphere cells are commonly used as a model of CSCs in 4T1 tumors [11]. The IC_{50} value of Sali-ABA in mammosphere 4T1-luc cells was 1.9 μM (95% CI=1.7~2.2 μM) (Figure 2B), which was significantly less than that in regular 4T1-luc cells. Thus, Sali-ABA maintained the selective toxicity towards CSCs.

Sali-ABA also showed selective toxicities to CSCs from a human breast cancer cell line, MDA-MB-231, a human colorectal cancer cell line, HCT-16, and a human prostate cancer cell line, PC-3 (Figure S1). In contrast, Sali-ABA is less toxic to normal epithelial cells than to carcinoma cells (Figure S2). These data together support the selective toxicity of Sali-ABA.

3.2 Generation and characterization of iTEP and iTEP-Sali-ABA conjugates

Since nanocarriers facilitate tumor accumulation of their drug payloads through the EPR effect [26, 27], we aimed to generate a nanocarrier and use it to deliver Sali-ABA to tumors. Our previous results showed an amphiphilic conjugate consisting of a hydrophilic iTEP and hydrophobic Sali (LogD 3.24 at pH 7.4, by MarvinSketch) self-assembled into NPs driven by its segmented amphiphilicity [2]. We wondered whether a conjugate between a hydrophilic iTEP and Sali-ABA would also possess sufficiently segmented amphiphilicity and assume a NP structure since Sali-ABA (LogD 7.34, pH 7.4) is more hydrophobic than Sali. To answer this question, we modified a previously established iTEP and generated a new hydrophilic iTEP having the sequence NH2-$(GAGVPG)_{70}$-$(CGGGGGGGG)_8$-COOH. The eight cysteines offered eight conjugation sites for Sali-ABA at one end of the iTEP. Eight-glycine spacers were inserted in between two adjacent cysteines so that each cysteine had ample space to accommodate a Sali-ABA molecule. The new iTEP was generated as a recombinant protein from *E. coli* cells. Purified iTEP migrated as a band between the 30 kDa and 46 kDa markers on SDS-PAGE, which was consistent with the theoretical molecular weight of the iTEP, 35.2 KDa (Figure 3A).

The iTEP was linked with Sali-ABA through MPBH. The ratio of Sali-ABA and iTEP in the purified iTEP-Sali-ABA conjugate was estimated to be 3:1. The release half-life of Sali-ABA from the conjugate was 12.15 hours (95% CI=9.98~15.52 hours) at pH 5.0 (Figure 3B). In contrast, there was no detectable release of Sali-ABA at neutral pH up to 100 hours. The pH-dependent release is as expected for a hydrazone linker and demonstrates the desired controlled release of Sali-ABA from the conjugate.

iTEP-Sali-ABA possessed a cytotoxicity 2.6 times lower than Sali-ABA when they were used to treat regular 4T1-luc cells (Figure 3C). The IC_{50} values of iTEP-Sali-ABA and Sali-ABA were 42.2 μM (95% CI 39.0~45.6 μM) and 16.4 μM (95% CI=14.3~18.8), respectively. However, iTEP-Sali-ABA was about eight times more toxic to mammosphere 4T1-luc cells (CSCs) than to regular 4T1-luc cells, resembling the selective toxicity of Sali-ABA and Sali (Figure 3D). The IC_{50} value of the iTEP-Sali-ABA in mammosphere 4T1-luc cells was 5.8 μM (95% CI= 5.4~6.2 μM), and the value in regular 4T1-luc cells was 42.2 μM.

The unmodified iTEP had a hydrodynamic diameter of 6.63±1.25 nm at 37 °C according to our DLS analysis (Figure 3E), which was consistent with our expectation that the iTEP remained a monomer in aqueous solution. iTEP-Sali-ABA, on the other hand, displayed a diameter of 51.2±18.2 nm, suggesting that the conjugate assumed a NP structure, as designed. The size of iTEP-Sali-ABA is also suitable for accumulation in tumors through the EPR effect [28].

3.3 Pharmacokinetics and tissue distribution of iTEP-Sali-ABA

The pharmacokinetics of Sali-ABA and iTEP-Sali-ABA were compared after they were administered intravenously to mice at a dose of 20 mg/Kg Sali-ABA equivalent. Plasma concentrations of Sali-ABA were monitored for up to 24 hours after the administration of either conjugates (Figure 4A). The temporal changes of the concentrations were fitted to a two-compartment pharmacokinetics model. According to the fit, the AUC of Sali-ABA of the iTEP-Sali-ABA conjugate was 2967.0 μM•hour (95% CI=2244.0~3509.0 μM•hour), which was approximately 30 times greater than the AUC of the Sali-ABA conjugate (99.9 μM•hour (95% CI=47.1~132.2 μM•hour). Similarly, the elimination half-life of Sali-ABA after the iTEP-Sali-ABA administration was 35 times longer than free Sali-ABA administration (13.9 hours, 95% CI=9.9~24.8 vs. 0.4 hours, 95% CI=0.2 ~4.1). In summary, these comparative results support the notion that iTEP-Sali-ABA significantly retarded the systematic clearance of Sali-ABA.

The aforementioned slow clearance and particle size of iTEP-Sali-ABA could enable the conjugate to leverage the EPR effect and, therefore, more efficiently accumulate in tumors. Indeed, at 24 hours after administration of free Sali-ABA or iTEP-Sali-ABA NP to 4T1-luc tumored mice, the NP resulted in 3.4 fold more Sali-ABA accumulation in the tumors than free Sali-ABA (3.1±0.1 ID%/gram vs 0.9±0.1 ID%/gram, Figure 4B). At the same time, there was a reduction of Sali-ABA accumulation in the heart when iTEP-Sali-ABA NP was compared with free Sali, although the difference was not statistically significant (0.57±0.18 ID%/gram vs 0.86±0.11 ID%/gram, Figure 4C). The reduction may benefit the toxicity profile of the NP as the heart is an organ sensitive to Sali [29]. The Sali-ABA accumulations in the liver, spleen, lung and kidneys have various extents of increases due to iTEP-Sali-ABA NP (Figure 4D).

3.4 Inhibition of primary tumor growth and metastasis by iTEP-Sali-ABA NP

When iTEP-Sali-ABA NPs were assessed for their inhibition of the growth and metastasis of 4T1-luc orthotopic tumors, we found that the NP slowed primary tumor growth. The tumors treated by the NP were smaller than the PBS-treated tumors starting from day 2 after the treatments (day 9 after tumor inoculation) (Figure 5A, $P<0.05$, *t-test*). Free Sali-ABA (20 mg/KG), on the other hand, failed to slow tumor growth.

The NP effectively inhibited metastasis of 4T1-luc tumors evidenced by its drastic improvement of metastasis-free survival in comparison to PBS treatment (P=0.007, Log-rank; Figure 5B). No mice in the NP-treated group developed metastasis before they were sacrificed. In contrast, the median metastasis-free survival for the PBS-treated mice was only 23 days. Free Sali-ABA also inhibited metastasis, as less than half of the mice in this group

developed metastasis, and the median metastasis-free survival of this group was not reached before the mice were sacrificed. However, the inhibitory effect of Sali-ABA was weaker than that of the NP because some Sali-ABA-treated mice developed metastasis. In addition, the survival of the PBS control group and the Sali-ABA group were not statistically different (P=0.252).

The overall survivals of PBS- and Sali-ABA-treated mice were not different from each other; both had a median survival of 24 days (Figure 5C). iTEP-Sali-ABA, however, significantly improved overall survival with a median survival of 39 days (iTEP-Sali-ABA vs PBS, P=0.0012; iTEP-Sali-ABA vs Sali-ABA, p=0.0011 Log-rank).

It is noteworthy that although iTEP-Sali-ABA NP inhibited both primary tumor growth and metastasis, the inhibitory effect was not enough to lead to stabilization or shrinking of the primary tumors. Indeed, NP-treated mice were sacrificed because of large primary tumor burdens. To overcome this limitation of iTEP-Sali-ABA NP, we developed a combination therapy that incorporates Sali and paclitaxel (PTX) together.

3.5 Inhibition of primary tumor growth and metastasis by a combination therapy of iTEP-Sali-ABA NPs and PTX NPs

Since PTX delivered by a nanocarrier has better efficacy than free PTX [30], we took advantage of iTEP-Sali-ABA NPs and used them to deliver PTX in an encapsulated form. The resulting NP, termed PTX NP, had PTX and Sali-ABA at a ratio of 6.6 to 1. Given Sali-ABA was much less toxic than PTX to regular 4T1 cells (IC_{50s}: 16.4 μM versus 6.3 nM), the toxicity of iTEP-Sali-ABA NP as the carrier was negligible in comparison to PTX. We were able to load PTX in the NP at an efficiency of 84.6±1.25% ($n=3$). The PTX NP had a mean diameter of 85.09±31.64 nm (Figure S3) and released PTX with a half-life of 4.67 hours, (95% CI=4.03~5.55 hours, Figure S4). In addition, PTX NP treated-mice had less body weight loss when compared with free PTX treated mice (data not shown). Lastly, results of the *in vitro* cytotoxicity study showed that the PTX NP possessed greater cytotoxicity to regular 4T1-luc cells than to mammosphere 4T1-luc cells (Figure 6A). The IC_{50} values of the PTX NP in the two types of cells were 6.32 nM (%95 CI=5.5~7.3 nM) and 44.6 nM (%95 CI=37.8~52.6 nM), respectively.

PTX NP and iTEP-Sali-ABA NP exert the same level of inhibition to primary tumor growth. The mean tumor sizes of mice receiving these two treatments were indifferent up to day 15 after tumor inoculation. Then, there was a significant difference of tumor sizes between the two treatments (P<0.05, *t-test,* Figure 6B). However, the difference disappeared after day 25. The median metastasis-free survival of the PTX NP treated mice was 37 days, suggesting the metastasis-inhibition effect of PTX NP was not as effective as iTEP-Sali-ABA NP since the latter treatment completely halted metastasis during the 39-day observation period (Figure 6C). Indeed, the metastasis-free survival of the two treatment groups were statistically different (P=0.002).

A combination therapy consisting of both the iTEP-Sali-ABA NP and the PTX NP showed a superior inhibitory effect to primary tumors than the PTX NP or the iTEP-Sali-ABA NP monotherapies starting at the 29th day after tumor inoculation (Figure 6B). The combination

therapy is more effective at inhibiting metastasis than the PTX NP monotherapy (P=0.001). 11 of 14 mice treated by the combination therapy remained metastasis free even at the end of the study, 69 days post tumor inoculation. However, the combination therapy was not superior to the iTEP-Sali-ABA NP in inhibiting metastasis.

The combination therapy was able to further prolong the overall survival of treated mice as compared to the PTX NP monotherapy and the iTEP-Sali-ABA NP monotherapy. The median overall survival of the combination therapy group was 69 days, while survival for PTX NP and iTEP-Sali-ABA NP therapy groups were only 41 days and 39 days (Figure 6D, P<0.001 in either comparison).

4. Discussion

In this study, we developed iTEP-Sali-ABA NP and demonstrated its ability to deliver Sali in a conjugated form and release it in a pH-dependent manner. Delivery of Sali in this NP was found to be an improvement over free Sali and was capable of preventing metastasis from orthotopic breast tumors. However, the NP did not inhibit the primary tumor growth. To address this limitation, iTEP-Sali-ABA NP was used in combination with PTX that was encapsulated in the NP. The combination therapy extended survival of the treated mice. We will discuss below key features embedded in the NP and this study that bestowed these benefits. We will also offer ideas for further improving these designs.

First, Sali was loaded to the iTEP carrier through a pH-sensitive hydrazone bond. To create this bond, we modified Sali so that the derivative, Sali-ABA, can react with MPBH to form a hydrazone and subsequently connect with the iTEP. We found the resultant conjugate (iTEP-Sali-ABA) to have ~10% of the toxicity of Sali (IC_{50}s: 42.2 μM vs 4.4 μM). There are at least two possible reasons that can be account for the decrease in toxicity: 1) Sali-ABA was not released from the NP completely, and 2) the modified carboxylic group of Sali (necessary for the ABA modification) affects the toxicity. The loss of the toxicity, however, is outweighed by the benefits of the NP carrier, including greater plasma AUC, higher intratumor accumulation, and a higher tolerable dose of Sali-ABA (30 mg/Kg for iTEP-Sali-ABA versus 5 mg/KG for Sali). Overall, the iTEP-Sali-ABA NP was more efficacious than Sali. Importantly, the NP enabled Sali to prevent metastasis. Together, these improvements not only validate the idea of using carriers to enhance the anti-metastasis effect of Sali, but also underscore the importance of drug carriers in general [31]. The delivery strategy in this study, nevertheless, may be improved by using a more potent Sali derivative and using a more environment-responsive bond connecting Sali to its carriers that allows for a greater extent of Sali release in tumor cells.

Second, iTEPs were used as building materials for the iTEP-Sali-ABA NP. There are three properties of iTEPs that benefit the NP[2]. First, iTEPs are humorally tolerated and do not elicit antibody responses. This is critical as antibody responses would severely compromise the activity of pharmaceuticals it they are immunogenic [32, 33]. The issue is especially prominent after multiple dosing of immunogenic pharmaceuticals. In contrast, repeatedly dosing the iTEP-Sali-ABA NP should not be an issue. Second, iTEPs are biodegradable. The NP will be eliminated from the body and thus should not cause toxicity as a result of the

long-term accumulation. Last, iTEPs are recombinant proteins. Their sequences and physicochemical properties such as hydrophobicity, conjugation sites (cysteines), and spacer length between the conjugation sites are precisely controlled using genetic engineering [20]. Using genetic engineering, we generated a series of iTEPs in this study that differ in the number of cysteine residues. We picked one iTEP which exhibited a good yield and gave the highest drug-to-carrier ratio. Using genetic engineering approach, it is easy to generate new iTEP carriers with the desired properties to deliver other CSC inhibitors if needed. This approach may also prove beneficial for creating an new iTEP-Sali-ABA NP that incorporates protein-based CSC-targeting molecules such as antibodies or peptides recognizing CSCs [34].

Third, there is a synergy between Sali and the iTEP-Sali-ABA NP that is built on the selective toxicity of Sali and the ability of the NP to deliver Sali to CSCs. The selective toxicity was reported previously [11]. However, it was the NP that translated the toxicity into a potent metastasis-inhibition effect, as the free Sali-ABA was not as effective. More significantly, the inhibitory effect was manifest in an orthotopic metastasis model. As this model has more clinical relevancy than other models used in previous Sali publications, the metastasis inhibition reported here is more clinically relevant [13]. The selective toxicity of Sali is also very critical to the function of the NP. The selective toxicity enabled the NP to completely block metastasis at a dose that failed to inhibit primary tumor growth. The selective toxicity also allowed safe usage of the NP even though there was considerable accumulation of Sali-ABA in the liver, spleen, and some other healthy organs. In summary, the synergy between Sali and the NP resulted in a metastasis-inhibition effect that has not been reported [19].

Last, a rationally designed combination therapy that consists of the NP-delivered Sali and PTX strikingly improved the overall survival and the metastasis-free survival for mice bearing 4T1 tumors, a very aggressive metastatic tumor [35]. The improvement is noteworthy as the survival results reported here are comparable or superior to recent therapeutic results reported in 4T1 metastasis models [36-38]. There are at least two intertwined reasons to use a combination therapy to tackle metastasis: (1) tumors include both differentiated tumor cells and CSCs, and the two cell populations interact with each other to propel tumorigenesis and metastasis [7], and (2) the two populations of cells have different drug susceptibility suggesting an effective therapeutic outcome may only be achieved by treating each of these populations with distinct drugs. To this end we have combined the metastasis inhibitor Sali with PTX for the treatment of the differentiated tumor cells. Thus, this combination therapy was a straightforward idea to simultaneously halt tumor growth and metastasis. Although this drug combination has been reported previously, [18], our study is distinct for the following three reasons. First, our study provided the first evidence that this drug combination is effective in inhibiting metastasis. Second, the results of our study clearly show the combination therapy is better than monotherapy in inhibiting metastasis and extending the overall survival of tumor-bearing animals. Third, both PTX and Sali used in our study were delivered by NP carriers, which we postulate led to the superior effect of our combination therapy. Future combination therapies will be benefited by a more sophisticated and stable formulation of PTX such as the one reported recently [39], and a

more potent formulation for Sali. Our combination therapy will also need to be examined in more sophisticated metastasis animal models and cancer patients.

Overall, our results show iTEP-ABA-Sali NP is a promising anti-metastasis therapeutic with desirable pharmacokinetics and tumor accumulation. These results underscore the benefits of using the combinational Sali/PTX therapy to treat malignant breast cancer and highlight the importance of drug carriers in cancer therapy.

Supplementary Material

Refer to Web version on PubMed Central for supplementary material.

Acknowledgements

We appreciate the technical suggestions from Drs. Jindrich (Henry) Kopecek, Pavla Kopeckova, and Jane Yang. We thank Dr. Sung Wan Kim for the DLS instrument, Mr. Xiangyang Ye for statistical analysis consultation, and Dr. Andrew Dixon for reviewing the manuscript. This research is supported by an NIH grant 4R00CA153929 and a University of Utah startup fund.

Reference

1. Mehlen P, Puisieux A. Metastasis: a question of life or death. Nat Rev Cancer. 2006; 6(6):449–58. [PubMed: 16723991]
2. Zhao P, et al. iTEP nanoparticle-delivered salinomycin displays an enhanced toxicity to cancer stem cells in orthotopic breast tumors. Mol Pharm. 2014; 11(8):2703–12. [PubMed: 24960465]
3. Scully OJ, et al. Breast Cancer Metastasis. Cancer Genomics - Proteomics. 2012; 9(5):311–320. [PubMed: 22990110]
4. Li F, et al. Beyond tumorigenesis: cancer stem cells in metastasis. Cell Res. 2007; 17(1):3–14. [PubMed: 17179981]
5. Al-Hajj M, et al. Prospective identification of tumorigenic breast cancer cells. Proc Natl Acad Sci U S A. 2003; 100(7):3983–8. [PubMed: 12629218]
6. Liu H, et al. Cancer stem cells from human breast tumors are involved in spontaneous metastases in orthotopic mouse models. Proc Natl Acad Sci U S A. 2010; 107(42):18115–20. [PubMed: 20921380]
7. Luo M, Brooks M, Wicha MS. Epithelial-mesenchymal plasticity of breast cancer stem cells: implications for metastasis and therapeutic resistance. Curr Pharm Des. 2015; 21(10):1301–10. [PubMed: 25506895]
8. Li X, et al. Intrinsic resistance of tumorigenic breast cancer cells to chemotherapy. J Natl Cancer Inst. 2008; 100(9):672–9. [PubMed: 18445819]
9. Diehn M, et al. Association of reactive oxygen species levels and radioresistance in cancer stem cells. Nature. 2009; 458(7239):780–3. [PubMed: 19194462]
10. Bao S, et al. Glioma stem cells promote radioresistance by preferential activation of the DNA damage response. Nature. 2006; 444(7120):756–60. [PubMed: 17051156]
11. Gupta PB, et al. Identification of Selective Inhibitors of Cancer Stem Cells by High-Throughput Screening. Cell. 2009; 138(4):645–659. [PubMed: 19682730]
12. Naujokat C, Steinhart R. Salinomycin as a drug for targeting human cancer stem cells. J Biomed Biotechnol. 2012; 2012:950658. [PubMed: 23251084]
13. Kopp F, et al. Salinomycin treatment reduces metastatic tumor burden by hampering cancer cell migration. Mol Cancer. 2014; 13:16. [PubMed: 24468090]
14. Boehmerle W, Endres M. Salinomycin induces calpain and cytochrome c-mediated neuronal cell death. Cell Death Dis. 2011; >2:e168. [PubMed: 21633391]

15. Story P, Doube A. A case of human poisoning by salinomycin, an agricultural antibiotic. N Z Med J. 2004; 117(1190):U799. [PubMed: 15107902]
16. Ojo OO, Bhadauria S, Rath SK. Dose-dependent adverse effects of salinomycin on male reproductive organs and fertility in mice. PLoS One. 2013; 8(7):e69086. [PubMed: 23840907]
17. Wei X, et al. Hyaluronic acid-based nanogel-drug conjugates with enhanced anticancer activity designed for the targeting of CD44-positive and drug-resistant tumors. Bioconjug Chem. 2013; 24(4):658–68. [PubMed: 23547842]
18. Zhang Y, et al. The eradication of breast cancer and cancer stem cells using octreotide modified paclitaxel active targeting micelles and salinomycin passive targeting micelles. Biomaterials. 2012; 33(2):679–91. [PubMed: 22019123]
19. Yao HJ, et al. The effect of hyaluronic acid functionalized carbon nanotubes loaded with salinomycin on gastric cancer stem cells. Biomaterials. 2014; 35(33):9208–23. [PubMed: 25115788]
20. Cho S, et al. Immune-tolerant elastin-like polypeptides (iTEPs) and their application as CTL vaccine carriers. Journal of Drug Targeting.
21. Roche. Lab FAQs: Find a Quick Solution (4th). 2013
22. Tao K, et al. Imagable 4T1 model for the study of late stage breast cancer. BMC Cancer. 2008; 8(1):228. [PubMed: 18691423]
23. Sheng X, et al. Isolation and enrichment of PC-3 prostate cancer stem-like cells using MACS and serum-free medium. Oncol Lett. 2013; 5(3):787–792. [PubMed: 23426586]
24. Manuel Iglesias J, et al. Mammosphere formation in breast carcinoma cell lines depends upon expression of E-cadherin. PLoS One. 2013; 8(10):e77281. [PubMed: 24124614]
25. Zhou Y, Yang J, Kopecek J. Selective inhibitory effect of HPMA copolymer-cyclopamine conjugate on prostate cancer stem cells. Biomaterials. 2012; 33(6):1863–72. [PubMed: 22138033]
26. Matsumura Y, Maeda H. A New Concept for Macromolecular Therapeutics in Cancer Chemotherapy: Mechanism of Tumoritropic Accumulation of Proteins and the Antitumor Agent Smancs. Cancer Research. 1986; 46(12 Part 1):6387–6392. [PubMed: 2946403]
27. Fang J, Nakamura H, Maeda H. The EPR effect: Unique features of tumor blood vessels for drug delivery, factors involved, and limitations and augmentation of the effect. Adv Drug Deliv Rev. 2011; 63(3):136–51. [PubMed: 20441782]
28. Petros RA, DeSimone JM. Strategies in the design of nanoparticles for therapeutic applications. Nat Rev Drug Discov. 2010; 9(8):615–27. [PubMed: 20616808]
29. Bastianello SS, et al. A chronic cardiomyopathy in feedlot cattle attributed to toxic levels of salinomycin in the feed. J S Afr Vet Assoc. 1996; 67(1):38–41. [PubMed: 8786618]
30. Zhang Z, Mei L, Feng SS. Paclitaxel drug delivery systems. Expert Opin Drug Deliv. 2013; 10(3): 325–40. [PubMed: 23289542]
31. Peer D, et al. Nanocarriers as an emerging platform for cancer therapy. Nat Nano. 2007; 2(12): 751–760.
32. Kontos S, Hubbell JA. Drug development: longer-lived proteins. Chem Soc Rev. 2012; 41(7):2686–95. [PubMed: 22310725]
33. De Groot AS, Scott DW. Immunogenicity of protein therapeutics. Trends Immunol. 2007; 28(11): 482–90. [PubMed: 17964218]
34. Deonarain MP, Kousparou CA, Epenetos AA. Antibodies targeting cancer stem cells: A new paradigm in immunotherapy? mAbs. 2009; 1(1):12–25. [PubMed: 20046569]
35. Pulaski BA, Ostrand-Rosenberg S. Mouse 4T1 breast tumor model. Curr Protoc Immunol. 2001; 20:20–2. Chapter. Unit.
36. Mastria EM, et al. Doxorubicin-conjugated polypeptide nanoparticles inhibit metastasis in two murine models of carcinoma. J Control Release. 2015; 208:52. [PubMed: 25637704]
37. Zhou M, et al. Radio-photothermal therapy mediated by a single compartment nanoplatform depletes tumor initiating cells and reduces lung metastasis in the orthotopic 4T1 breast tumor model. Nanoscale. 2015

38. Gao ZG, et al. Prevention of metastasis in a 4T1 murine breast cancer model by doxorubicin carried by folate conjugated pH sensitive polymeric micelles. J Control Release. 2011; 152(1):84–9. [PubMed: 21295088]

39. Bhattacharyya J, et al. A paclitaxel-loaded recombinant polypeptide nanoparticle outperforms Abraxane in multiple murine cancer models. Nat Commun. 2015; 6:7939. [PubMed: 26239362]

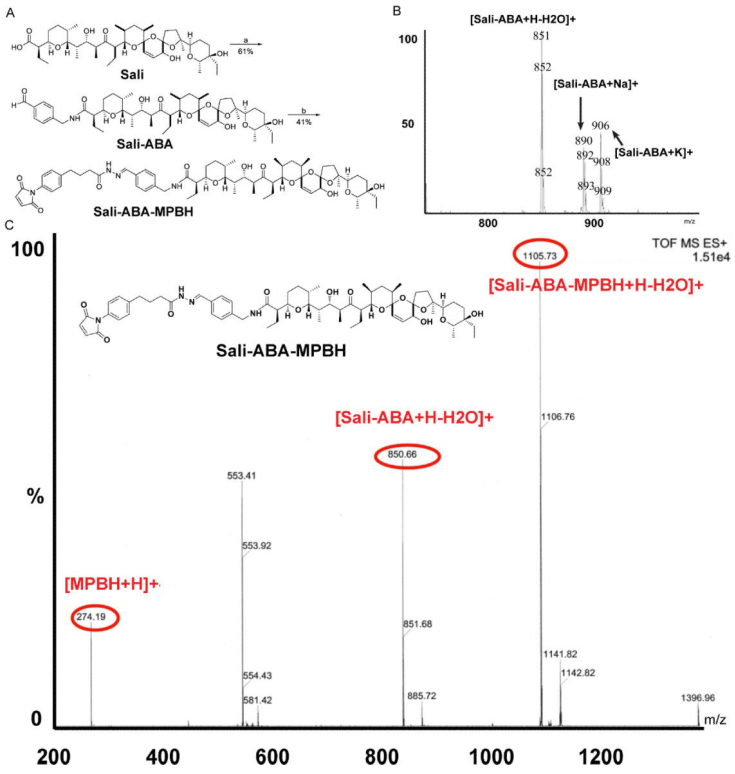

Figure 1.

A. The synthesis scheme of Sali-ABA and Sali-ABA-MPBH. **B**. An ESI-MS spectrum of a purified reaction product between ABA and Sali. Several major molecular ion peaks are labelled. **C.** An ESI-MS spectrum of purified reaction product between Sali-ABA and MPBH. The insert is the expected chemical structure of the Sali-ABA-MPBH conjugate. The peak that matches the MW of Sali-ABA-MPBH is evident. The presence of peaks of MPBH and Sali-ABA of this purified conjugate suggests that the hydrazone bond inside the conjugate is not stable under the ESI-MS experimental conditions.

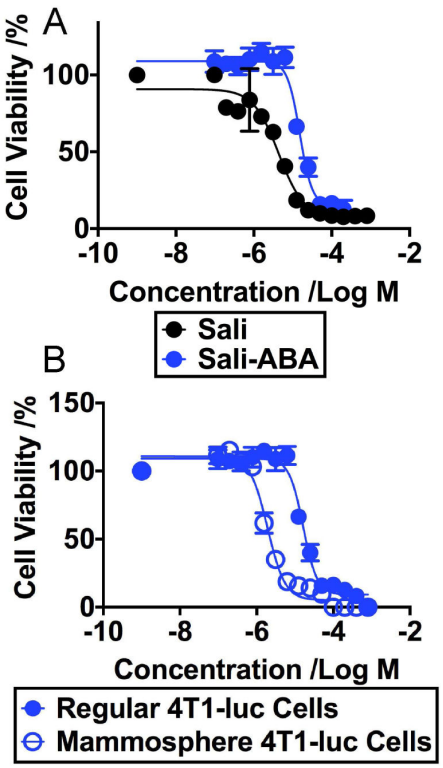

Figure 2.

A. The viability profile of regular 4T1-luc cells after they were exposed to different concentrations of Sali or Sali-ABA for 72 hours. The IC_{50} values of Sali and the Sali-ABA are statistically different ($P< 0.0001$, *t-test*). **B.** The viability profile of regular 4T1-luc cells versus mammosphere 4T1-luc cells after they were exposed to different concentrations of Sali-ABA for 72 hours. The IC_{50} values of Sali-ABA in regular 4T1–luc and mammosphere 4T1-luc are statistically different ($P<0.0001$ *t-test*).

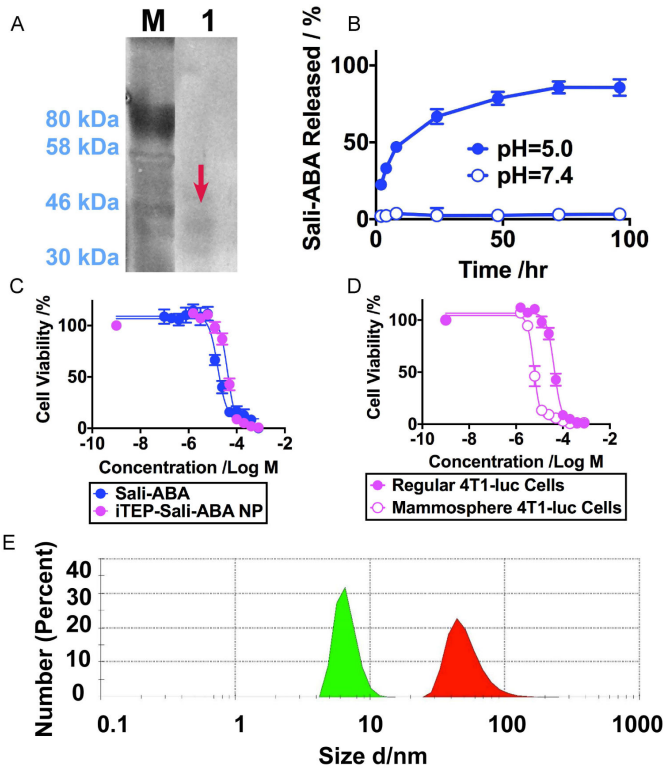

Figure 3.

A. A copper-stained SDS-PAGE photo of purified iTEPs after 10 rounds of purification. The loading amount was 50 μg/well. The band is highlighted with a red arrow. **B.** The *in vitro* release profile of iTEP-Sali-ABA NP at pH=5.0 (0.1 M acetate buffer) and pH=7.0 (PBS). **C.** The viability profile of regular 4T1-luc cells after they were exposed to different concentrations of iTEP-Sali-ABA NP or Sali-ABA for 72 hours. The IC_{50} values of iTEP-Sali-ABA NP and Sali-ABA in regular 4T1-luc cells are statistically different ($P<0.0001$, *t-test*). **D.** The viability profile of regular 4T1-luc cells versus mammosphere 4T1-luc cells after they were exposed to different concentrations of iTEP-Sali-ABA NP for 72 hours. The two types of cells have statistically different IC_{50} values ($P<0.0001$, *t-test*). **E.** Hydrodynamic diameters of the unconjugated iTEP (green filled area) and iTEP-Sali-ABA NP (red filled area). The sample concentrations were 25 μM. The unconjugated iTEP was reduced in 100 mM TCEP solution overnight before the measurement.

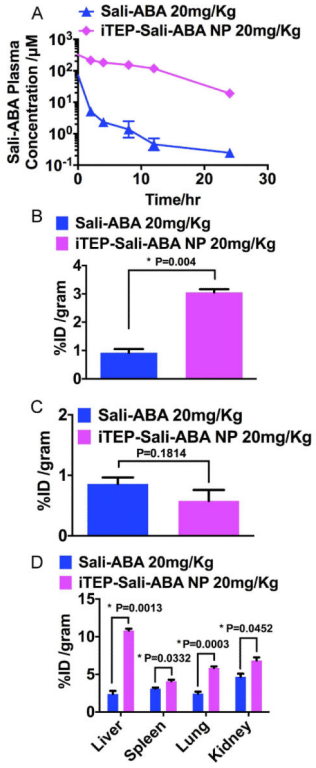

Figure 4.

A. Plasma concentration of Sali-ABA after it was administered in its free form or iTEP-Sali-ABA NP. **B.** Tumor accumulation of Sali-ABA after it was administered at 20 mg/kg dose (same below). Tumors and all following organ samples were collected at 24 hours post administration. The quantities of Sali-ABA were expressed as percentage of initial dose normalized by weight of organs, ID% /gram. The data were analyzed by one-way ANOVA. P-value is shown in the figure and * indicates a significant difference. **C.** Heart accumulation of Sali-ABA. The data were analyzed by one-way ANOVA. P-value is shown in the figure. **D.** The accumulation of Sali-ABA in livers, spleens, lungs, and kidneys. The data were analyzed by one-way ANOVA. P-values are shown in the figure and * indicates a significant difference.

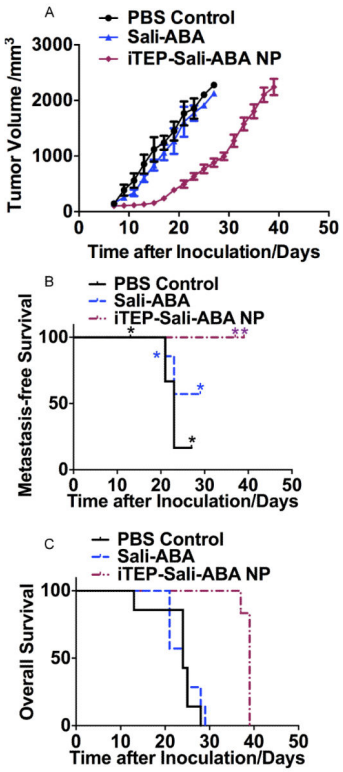

Figure 5.

A. The volume change of 4T1-luc orthotopic tumors after they were treated by PBS, free Sali-ABA, or iTEP-Sali-ABA NP. **B.** The metastasis-free survival of mice bearing 4T1-luc orthotopic tumors after they were treated as described in 5A. * indicates the time points when some mice were censored because they reached humane endpoints. The metastasis-free survival of the NP-treated mice is significantly longer than PBS-treated mice (P=0.007, Log-rank test). **C.** The overall survival profile of mice described in 5A. The overall survival of the NP-treated mice is significantly longer than both Sali-ABA- and PBS-treated mice (P=0.0011 and 0.0012 respectively, Log-rank test).

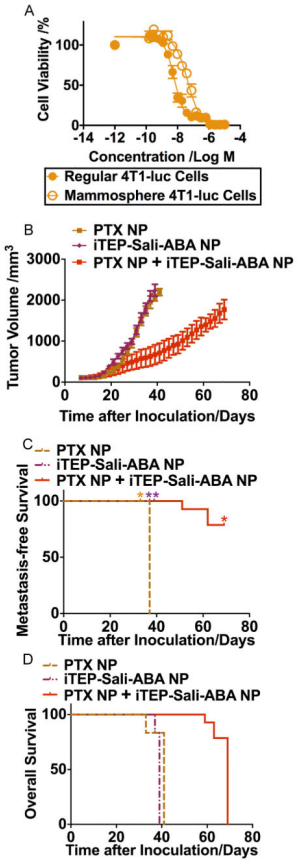

Figure 6.

A. Viability profile of regular 4T1-luc cells and mammosphere 4T1-luc cells after they were treated by PTX NP for 72 hours. The two IC_{50} values are statistically different (P<0.0001, *t-test*). **B.** The volume changes of 4T1-luc orthotopic tumors after they were treated by iTEP-Sali-ABA NP, PTX NP, or a combinational regimen of PTX NP and iTEP-Sali-ABA NP. **C.** The metastasis-free survival of mice bearing 4T1-luc orthotopic tumors after they were treated as described in 6B. * indicates the time points when some mice were censored because they reached humane endpoints. The metastasis-free survival of the iTEP-Sali-ABA NP-treated mice is significantly longer than the PTX NP-treated mice (P=0.002, Log-rank test). The metastasis-free survival of the combination therapy-treated mice is significantly longer than the PTX NP-treated mice (P=0.001, Log-rank test). **D.** The overall survival profile of mice described in 6B. The overall survival of the combination therapy-treated mice is significantly longer than both iTEP-Sali-ABA NO- and PTX NP-treated mice (P<0.001 in both cases, Log-rank test).